

# Apparent thermal conductivity of evacuated $\text{SiO}_2$ -aerogel tiles under variation of radiative boundary conditions

P. SCHEUERPFLUG, R. CAPS, D. BÜTTNER and J. FRICKE

Physikalisches Institut, Universität Würzburg, Am Hubland, D-8700 Würzburg, F.R.G.

(Received 15 February 1985)

**Abstract**—The apparent thermal conductivity  $\lambda$  of evacuated  $\text{SiO}_2$ -aerogel tiles was measured with our small guarded hot plate vacuum system LOLA II. In order to study the influence of the boundary emissivity on  $\lambda$  the plates ( $20 \times 20 \text{ cm}^2$ ) were either used with their plasma-sprayed surfaces ( $\epsilon \approx 0.5$ ) or with low-emissivity aluminum ( $\epsilon \approx 0.05$ ) foils as covers. The difference in the apparent conductivity already showed at room temperature and rose to about 50% for radiative temperatures  $T_r = 570 \text{ K}$ . An important consequence is that superinsulating  $\text{SiO}_2$ -aerogel systems should always be provided with low-emissivity boundaries around the aerogel. The calorimetric results for  $\lambda$  are compared with radiative conductivity values derived from spectral i.r. transmission measurements.

## 1. INTRODUCTION

THERE ARE two main possibilities to improve the thermal insulation of double-pane window systems: radiative losses can be considerably reduced if the panes are covered with low-emissivity layers. In order to suppress convection and conduction the space between the panes would have to be evacuated. This is not feasible without rigid supports as the panes would fracture under the external atmospheric pressure load. The situation changes if transparent and highly porous silica-aerogel tiles were to be used as a rigid spacer. In order to pursue such a possibility data on the optical transparency [1] and the insulating properties of aerogel have to be collected.

The apparent thermal conductivity  $\lambda$  of evacuated  $\text{SiO}_2$ -aerogel tiles has been measured recently [2] in our large guarded hot plate system LOLA I. With 'black' boundaries (large i.r. emissivities) the effective  $\lambda$  for a 22-mm-thick aerogel tile is as low as  $8 \times 10^{-3} \text{ W m}^{-1} \text{ K}^{-1}$  at  $T_r \approx 280 \text{ K}$  but rises to about  $25 \times 10^{-3} \text{ W m}^{-1} \text{ K}^{-1}$  at  $T_r \approx 380 \text{ K}$ . This increase is caused by radiation leakage in the weak absorption wavelength region below  $\Lambda = 8 \text{ } \mu\text{m}$  and especially in the transmission window below  $\Lambda = 5 \text{ } \mu\text{m}$ . This was revealed by measuring the spectral i.r. absorption of aerogel tiles and by solving the radiation transport equation [3].

If aerogel thus were to be used as superinsulating spacer not only in windows or in covers for low temperature passive solar use but also in evacuated solar collectors, the i.r. radiation transport would have to be diminished. This could be attained by increasing the i.r. extinction within the aerogel tiles or/and by reducing the i.r. emission from the boundaries around the aerogel. Experimental and theoretical values for the apparent thermal conductivity under variation of boundary emissivity are presented and discussed in this report [4].

## 2. EXPERIMENTAL SET-UP AND RESULTS

Aerogel tiles of sizes  $160 \times 160 \times 22 \text{ mm}^3$  and of density  $\rho \approx 100\text{--}110 \text{ g dm}^{-3}$  were inserted into our small guarded hot plate system LOLA II (Fig. 1). It is suitable for thermal conductivity measurements up to temperatures of  $800^\circ\text{C}$  and allows for mechanical load variations onto the evacuated samples of up to 50 bar. Its principal use is to determine the load dependence of the solid conductivity of fiber or powder insulations [5]. For the aerogel measurements the external load was varied only up to 1 bar, which was enough to guarantee proper solid contact between the tiles and the plates. The vacuum in the hot plate system was always below  $10^{-6} \text{ mbar}$ . The temperature  $T_H$  of the hot plate was varied between 40 and  $400^\circ\text{C}$ . The temperature difference  $\Delta T = T_H - T_C$  between the hot plate and the colder reference plates was between 20 and 30 K. The measured thermal conductivities are presented as function of the average temperature  $T_r$ , with  $T_r^3 = (T_H^3 + T_C^3) \cdot (T_H + T_C)/4$ . The outer rims of the aerogel tiles had to be carefully shielded thermally by a reflecting aluminum foil and adjacent fiber insulations. Otherwise a strong i.r. flux is radiated not only off the rims of the aerogel tiles but also off their inner volumina—due to the low optical thickness below  $8 \text{ } \mu\text{m}$ . Without these precautions this loss flux could easily be many times as strong as the 'main' flux between the hot plate and the reference plates. With proper shielding the losses amounted to about 30% at the highest temperature ( $T_r = 570 \text{ K}$ ). These losses were determined by additionally adjusting hot plate and reference plates to the same temperature  $T = T_r$  and measuring the power input into the central section of the hot plate.

It should be mentioned that for all aerogel applications it is important to reduce the radiative losses by using boundaries with low emissivities.

The effect of the emissivity of the hot plate and the

NOMENCLATURE

$d$	sample thickness	$T_r$	average radiation temperature
$E$	extinction coefficient	$x$	depth.
$e_b$	total black-body emissive power	Greek symbols	
$e_{\Lambda,b}$	spectral black-body emissive power		
$f_R$	Rosseland mean weight function	$\epsilon$	emissivity
$n$	index of refraction	$\epsilon'$	effective emissivity
$N_1$	conduction-radiation parameter	$\Lambda$	wavelength
$q$	total heat flux	$\lambda$	total (apparent) thermal conductivity
$q_s$	solid conduction heat flux	$\lambda_s$	solid conductivity
$q_r$	radiative heat flux	$\lambda_r$	radiative conductivity
$Q_R$	dimensionless radiative flux	$\rho$	density
$T$	temperature	$\tau_0$	optical thickness
$T_H, T_C$	temperature of hot, cold boundary	$\sigma$	Stefan-Boltzmann constant.

reference plates on the apparent conductivity was investigated by first using plasma-sprayed surfaces with  $\epsilon \approx 0.5$  in the i.r. region and afterwards repeating the measurements with an aluminum foil ( $\epsilon \approx 0.05$ ) as a cover on the plates. The emissivities were determined with a radiation thermometer (KT4-Heimann).

The apparent  $\lambda$ -values for the 22-mm aerogel tiles are depicted in Fig. 2. They are accurate to within 5%. As our data show for  $T_r = 570$  K,  $\lambda$  can be reduced by a factor of two if low-emissivity boundaries are used. For glass panes with  $\epsilon$  close to 1 the effect of low emissivity  $\text{In}_2\text{O}_3$  layers would be even more pronounced.

3. OPTICAL AND i.r. PROPERTIES OF AEROGEL

Aerogel is transparent in most of the visible part of the spectrum. Due to small particle diameters and pores in the order of 10 nm, however, Rayleigh scattering occurs for small wavelengths, especially for blue light [1]. In the i.r. spectral region aerogel only absorbs radiation. The absorption coefficient is similar to that one of fused silica, with strong absorption above  $\Lambda = 8 \mu\text{m}$  (up to  $40 \mu\text{m}$ ), medium absorption between 5 and  $8 \mu\text{m}$  and low absorption below  $5 \mu\text{m}$  as shown in

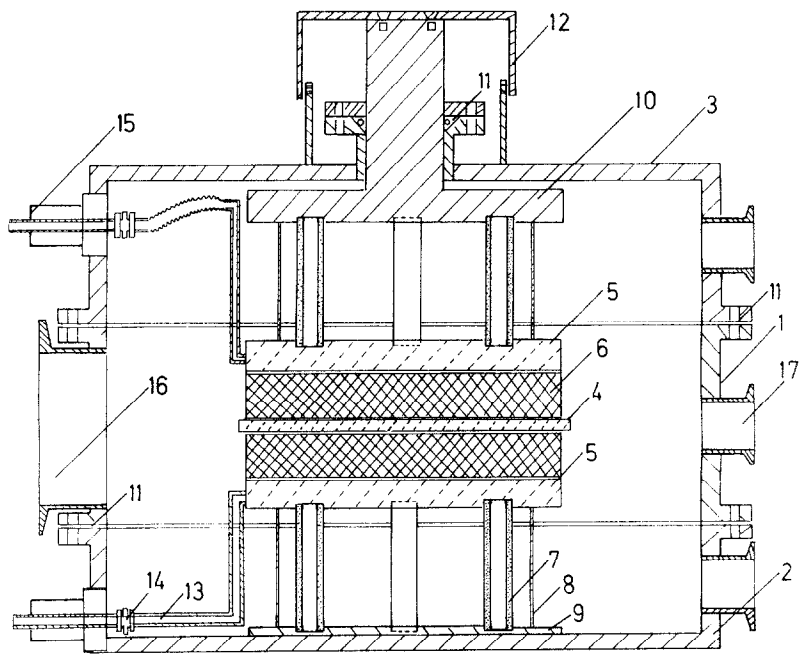


Fig. 1a. Guarded hot plate vacuum system LOLA II. The numbers refer to the following items: 1-3, vacuum chamber; 4, hot plate with two guard rings; 5, reference plates; 6, aerogel samples; 7, ceramic insulating tubings; 8, thin metal connectors; 9, bottom plate; 10, piston; 11, vacuum seal; 12, holder for piston; 13-15, parts for cooling; 16 and 17, vacuum flanges.

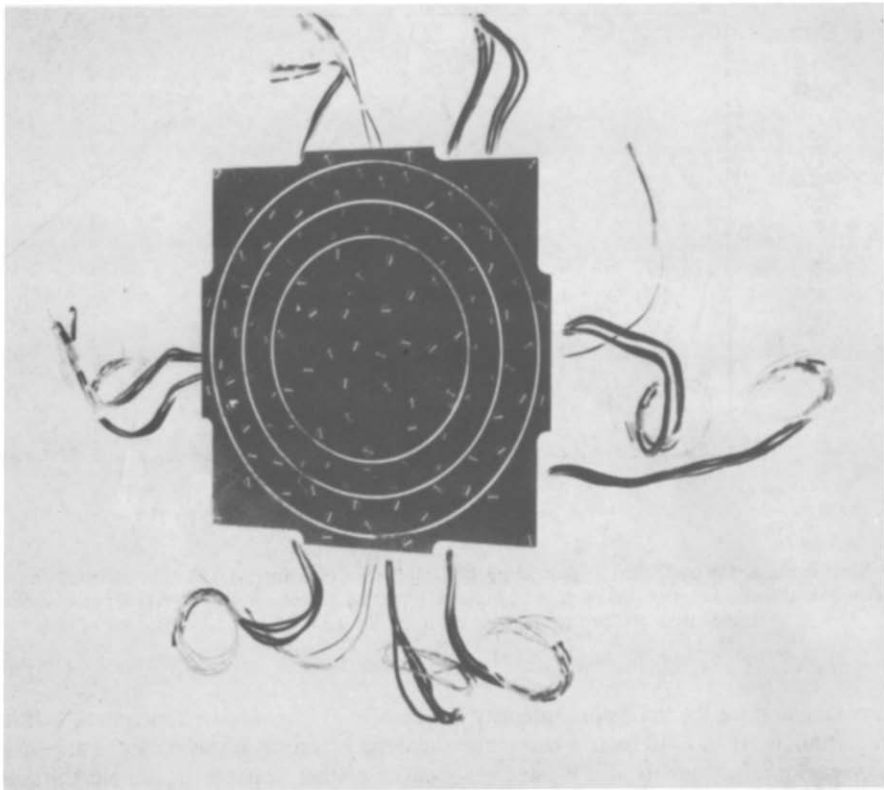


FIG. 1b. Hot plate system with central metering section, two guard rings and corner sections; the overall dimensions are about  $20 \times 20 \text{ cm}^2$ , 10 Pt100 thermo-resistors are distributed within the hot plate system. In the hot plate system 6.5 m of coaxial heater are used.

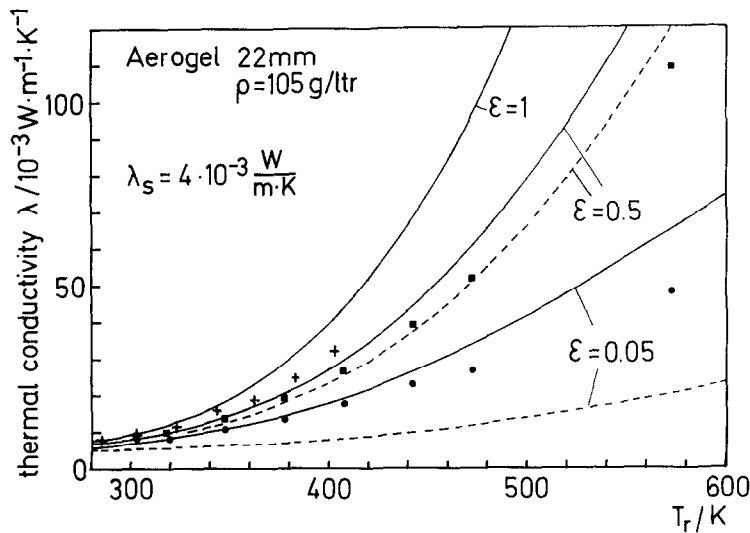


FIG. 2. Apparent thermal conductivities for 22-mm aerogel tiles with density  $\rho = 105 \text{ g dm}^{-3}$  under variation of average radiative temperature  $T_r$ ; ■ results from measurements for a boundary with  $\varepsilon \approx 0.5$ ; ● measurements for a highly reflecting boundary ( $\varepsilon \approx 0.05$ ); + measurements from LOLA I with high emissivity glass paper boundary around the aerogel tile [2]. The solid lines are the corresponding calculated pseudo-conductivities according to equation (8) using the concept of effective emissivities  $\varepsilon'$ , the dashed lines are calculated without the coupling of radiation and solid conduction [ $\varepsilon' = \varepsilon$  in equation (8)].

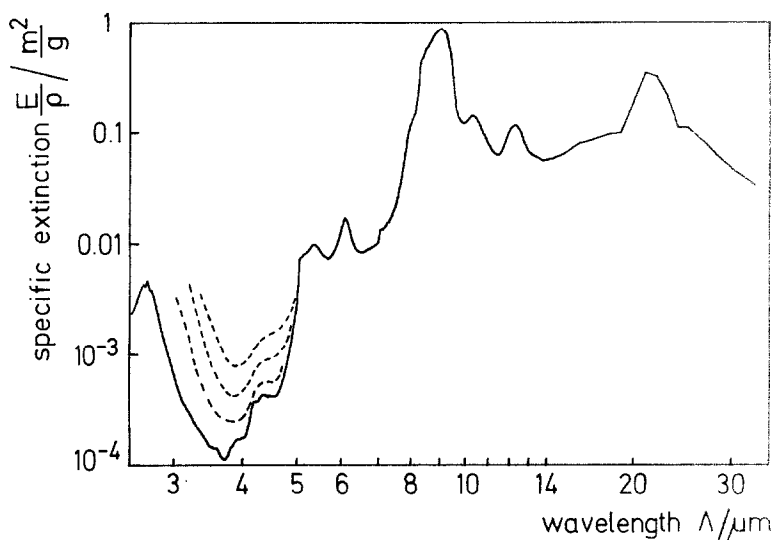


Fig. 3. Specific extinction coefficient  $E/\rho$  for aerogel. The influence of adsorbed water can especially be seen within the low absorption region below  $\lambda = 5 \mu\text{m}$ : solid line is for samples heated to  $400^\circ\text{C}$  under vacuum, dashed lines are for aerogel exposed to air for 0.5 h, 12 h and 2 days.

Fig. 3. At room temperature the maximum intensity of thermal radiation is at  $\lambda = 10 \mu\text{m}$ , where the large absorption region of aerogel is also located. A considerable part of the thermal radiation, however, may penetrate aerogel within the radiation window below  $5 \mu\text{m}$ . Here the i.r. transmission is strongly influenced by the water adsorbed by the aerogel skeleton. Water strongly absorbs i.r. radiation at  $3 \mu\text{m}$  (another absorption band occurs at  $\lambda = 6 \mu\text{m}$ ). In Fig. 3 the specific extinction coefficient  $E/\rho$  (with  $E$  = extinction coefficient,  $\rho$  = density) is shown for aerogel samples, which have been heated up to  $400^\circ\text{C}$  under vacuum (solid line below  $\lambda = 5 \mu\text{m}$ ) and then were exposed to air for 0.5 h, 12 h and 2 days (dashed lines). The extinction data up to  $\lambda = 15 \mu\text{m}$  have been determined with the apparatus described in [3], the data above  $\lambda = 15 \mu\text{m}$  have been derived from transmission measurements of fused silica in KBr with a convectional spectrometer.

Due to its high porosity the index of refraction  $n$  of the aerogel tiles is very low. It was determined to about  $n = 1.02$  with a He-Ne laser by a minimum deviation technique.

#### 4. THEORY OF HEAT TRANSFER IN AEROGEL

In all high temperature fiber or powder insulations tested in our hot plate systems so far (see for example [5, 6]) the optical thickness  $\tau_0 = E \cdot d$  (with  $d$  = sample thickness) was of the order of a few hundred. Thus it was possible to treat the radiative transport as a diffusion process and to add the solid conductivity  $\lambda_s$  and the radiative conductivity  $\lambda_r$  according to

$$\lambda = \lambda_s + \lambda_r = \lambda_s + (16/3) \cdot n^2 \cdot \sigma \cdot T_r^3 / E, \quad (1)$$

where  $\sigma$  is the Stefan-Boltzmann constant. Data analysis is simple in this case and the determined  $\lambda$ -values neither depend on sample thickness nor on boundary emissivity. The temperature profile is in between the linear case [solid conduction  $(T_H - T) \propto x$ , with  $x$  being the distance between hot plate and cold plate and  $T$  the temperature at position  $x$ ] and the hypothetical pure radiative case [ $(T_H - T)^4 \propto x$ ].

The simple form of equation (1), however, doesn't hold in silica-aerogel. This is due to the i.r. transmission window with values of  $\tau_0$  of the order of 1 for a 22-mm tile (Fig. 3). In this wavelength region radiative transport is not a local phenomenon any more, as some i.r. photons may completely penetrate the tiles and allow for direct radiative 'communication' between the boundaries. As a consequence the measured  $\lambda$ -values strongly vary with the sample thickness and the emissivity of the boundaries. In this case the coupling between the radiation field and the heat flux caused by solid conduction has to be taken into account. If one considers low-emissivity walls ( $\epsilon \approx 0.1$ ) the radiation flux close to the walls is weak. Further inside the aerogel increasingly more radiation is produced by i.r. emission. In order to conserve the total thermal flux the temperature gradient thus has to change across the aerogel tile: a more or less steep gradient is expected close to the boundaries, which enhances energy transport via solid conduction, while deep within the aerogel the gradient is small (Fig. 4). Here the contribution of solid conduction is reduced.

In an exact treatment the heat transfer for combined radiation and conduction is described by a complicated integro-differential equation [7, 8]. It is in general dependent on the temperatures  $T_H$  and  $T_C$ , the emissivity  $\epsilon$  of the side walls, the amount of solid conduction compared to radiative conduction,

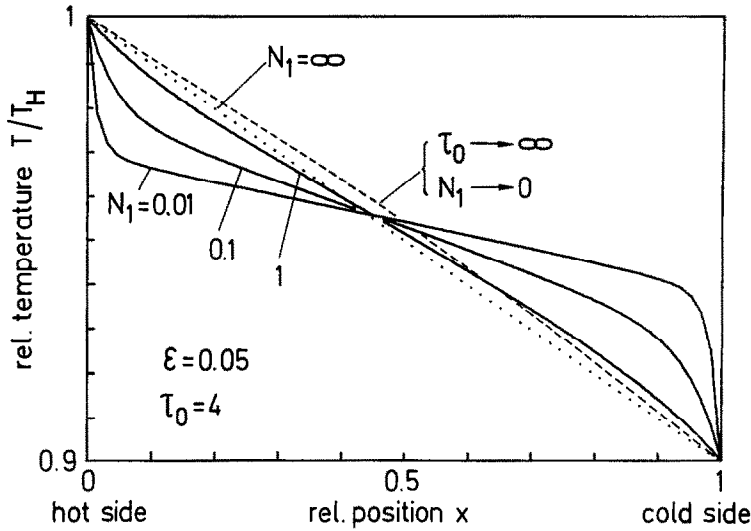


FIG. 4. Temperature profile for pure conduction ( $N_1 \rightarrow \infty$ , dotted line), the hypothetical case with pure radiative transport ( $N_1 = 0$ ,  $\tau_0 = \infty$ , dashed line) and temperature profiles for a medium with optical thickness  $\tau_0 = 4$  and boundary emissivity  $\epsilon = 0.05$  for different conduction-radiation parameters  $N_1$  (solid lines).

described by the parameter  $N_1 = \lambda_s \cdot E / (4\sigma T_H^4)$ , and the optical thickness  $\tau_0(\lambda)$ . As it is very tedious to solve this integro-differential equation numerically for a non-gray medium as aerogel, we developed approximate analytical expressions for the total heat flux  $q$ .

A well-known approximation for the total heat flux  $q$  in a gray medium is the addition of solid conduction heat flux  $q_s$  and radiative heat flux  $q_r$  [compare with equation (1)]:

$$q = q_s + q_r = \lambda_s \cdot (T_H - T_C) / d + q_r \quad (2)$$

The radiative contribution  $q_r$  in a gray insulation with black boundaries ( $\epsilon = 1$ ) can be approximated by

$$q_r = n^2 \sigma \cdot (T_H^4 - T_C^4) / (1 + 3/4 \cdot \tau_0), \quad (3)$$

The above expression is exact for zero and large optical thickness  $\tau_0$  and correct within 4% for arbitrary  $\tau_0$ . The influence of the emissivity  $\epsilon$  in the case of pure radiative heat transport ( $N_1 = 0$ ) can be described by a similar equation [8]

$$q_r = n^2 \sigma \cdot (T_H^4 - T_C^4) / (2/\epsilon - 1 + 3/4 \cdot \tau_0). \quad (4)$$

This equation will give wrong results in the general case of non-zero solid conduction ( $N_1 > 0$ ) and emissivity  $\epsilon < 1$ , where a considerable amount of radiation emerges from layers near the boundary. Due to the strong temperature gradient near the wall (Fig. 4) the energy can effectively be delivered into the boundary layers via solid conduction.

The amount of radiation emitted from the boundary layer depends on its optical absorption thickness  $\tau$ . Furthermore, the lower the emissivity  $\epsilon$  of the walls for a given  $\tau$  the more radiation, compared to the emission of the walls, will proceed from the boundary layers into the aerogel tile. To take care of the boundary-layer

effect the emissivity  $\epsilon$  in equation (4) may be substituted by a (higher) effective emissivity  $\epsilon'$ .

In a zero-order approach this effective emissivity  $\epsilon'$  of the wall plus the boundary layer of optical thickness  $\tau$  can be derived from a semiempirical relation:

$$\epsilon' = 1 - (1 - \epsilon) \cdot \exp \{ -N_1 / (2 \cdot N_1 + 0.04) \} \times \arctan [\tau_0 \cdot (1 + 0.02/N_1)]. \quad (5)$$

For  $\epsilon = 1$  we get  $\epsilon' = 1$ , for  $\epsilon < 1$ , however,  $\epsilon' > \epsilon$  results. We restricted the boundary layer to a certain limit  $\tau'$ , a behavior which can be simulated by the introduction of the arctan function. We also included a suitable dependence of the argument on the conduction-radiation parameter  $N_1$  to get the correct results in the pure radiative case ( $N_1 = 0$ ). The free parameters were adjusted according to the results of an exact numerical calculation in a gray absorbing medium. The range of the optical thickness  $\tau_0$  was varied between 0.1 and 10, the emissivity  $\epsilon$  between 0.01 and 1.  $N_1$  was chosen either 10, 1, 0.1 or 0.01. By inserting the effective emissivity  $\epsilon'$  from equation (5) into (4) the approximate total flux  $q$  can be calculated with an error of about 5% in the average and maximum deviations of 15% compared to the exact numerical calculations. Compared to other approximate methods [9] the above empirical expression has a relatively simple form and includes the general case of arbitrary conduction-radiation parameter  $N_1$ . An alternative expression for the total heat flux  $q$  is given in [10], however, it yields large errors for the case  $\epsilon \ll 1$ .

If  $N_1$  is larger than 0.1, equation (5) can be simplified:

$$\epsilon' = 1 - (1 - \epsilon) \cdot \exp [ -\arctan (\tau_0) / 2 ]. \quad (6)$$

Furthermore in the case of large  $\tau_0$  ( $> 5$ ) and small

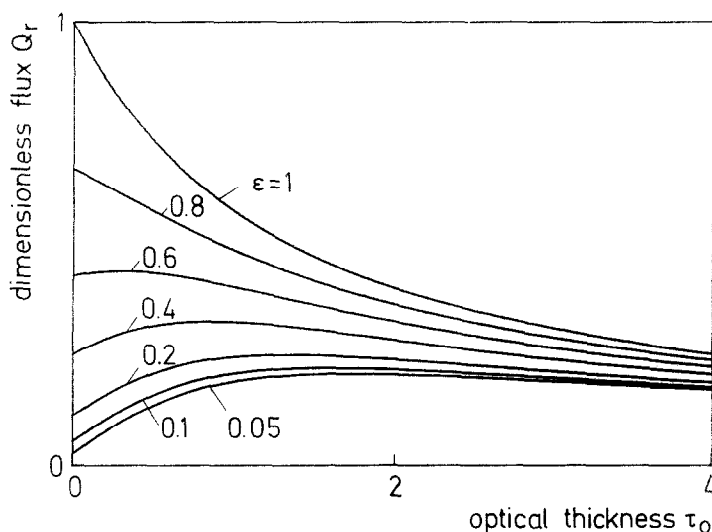


FIG. 5a. Dimensionless radiative flux  $Q_r$  according to equation (4) using the effective emissivity  $\epsilon'$  of (6) as a function of optical thickness  $\tau_0$ . The parameter is  $\epsilon$ , the emissivity of the walls. For low  $\epsilon$ -values the radiative flux increases with rising  $\tau_0$ !

emissivity  $\epsilon$  ( $< 0.2$ )  $\epsilon'$  becomes about 0.5 and the radiative flux according to (4) is

$$q_r = (4/3)n^2\sigma \cdot (T_H^4 - T_C^4)/(\tau_0 + 4). \quad (7)$$

The effective emissivity in equation (6) (with  $N_1 > 0.1$ ) was used to calculate the dimensionless radiative flux  $Q_r = q_r/[n^2\sigma \cdot (T_H^4 - T_C^4)]$  as a function of optical thickness  $\tau_0$  and wall emissivity  $\epsilon$  as shown in Fig. 5a. The remarkable result is that for low emissivity the radiative flux may become larger if the optical thickness  $\tau_0$  is increased! This is due to the coupling of radiation and solid conduction near the boundary. The same calculations for the case of pure radiative heat transport

[ $N_1 = 0$ , equation (4)] generally yield lower heat fluxes especially for low emissivities  $\epsilon$  as shown in Fig. 5b.

As the optical thickness in aerogel is strongly wavelength dependent (Fig. 3), equation (5) has to be generalized to a non-gray medium. The total emissive power  $e_b = \sigma T^4$  then is replaced by the spectral emissive power of a black body  $e_{\lambda,b}(T)$ . Assuming small temperature differences  $\Delta T = T_1 - T_2$  and integrating over all wavelengths the total flux  $q$  is given by

$$q = \lambda_s \cdot \Delta T/d + 4 \cdot n^2 \sigma T^3 \cdot \Delta T \times \int_0^\infty f_R(\Lambda, T)/[2/\epsilon'(\Lambda) - 1 + 3/4 \cdot \tau_0(\Lambda)] d\Lambda, \quad (8)$$

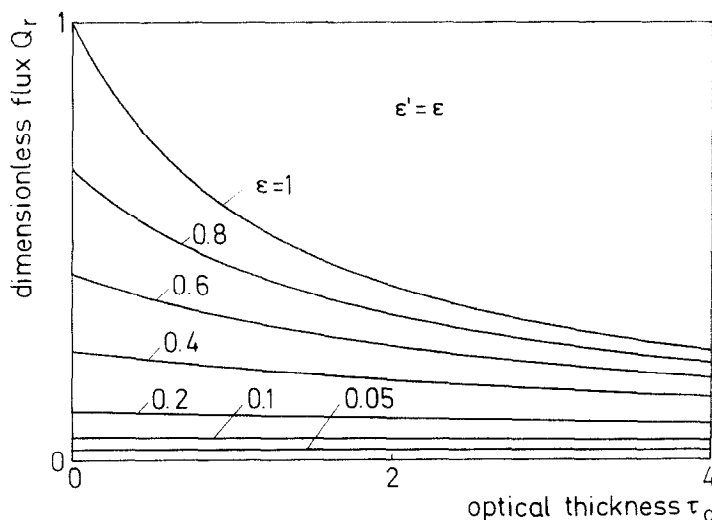


FIG. 5b. Dimensionless radiative flux  $Q_r$  according to equation (4) (pure radiative case) as function of optical thickness with parameter  $\epsilon$ . For small  $\epsilon$  the flux is considerably smaller than in Fig. 5a.

where  $\varepsilon'(\lambda)$  is calculated according to equation (5), however, using spectral optical thicknesses and emissivities.  $f_R(\lambda, T)$  is the Rosseland mean weight function [11], i.e. the change of spectral emissive power with total emissive power:  $\{\partial e_{\lambda,b}(T)/\partial e_b(T)\}_\lambda$ . For the conduction-radiation parameter  $N_1$  an average extinction coefficient  $E_{av}(T)$  has to be used. It was derived by comparing the dimensionless flux of a gray medium with extinction coefficient  $E_{av}$  to the radiative flux of the non-gray medium [equation (8)] with black boundaries:  $Q_r(\varepsilon = 1) = 1/[1 + (3/4) \cdot E_{av} \cdot d]$ .

Equation (8) and the optical data of Fig. 3 were used to calculate the pseudo-conductivity  $\lambda = q \cdot d/\Delta T$  of the aerogel tiles measured with LOLA II. The solid conductivity of aerogel was taken  $\lambda_s = 4 \text{ mW m}^{-1} \text{ K}^{-1}$ . The parameter  $N_1(T)$  of the aerogel tiles then varies between  $N_1 = 1$  at  $T = 300 \text{ K}$  to  $N_1 = 0.015$  at  $T = 600 \text{ K}$ . At higher temperatures thus radiation is the main channel for heat transfer in aerogel. For wall emissivities  $\varepsilon = 1, 0.5$  and  $0.05$  the results of the calculation are shown in Fig. 3. They agree well with the conductivity measurements of aerogel. The uncertainty of the theoretical results is estimated to be about  $\pm 20\%$  (including the uncertainty of the wall emissivity  $\varepsilon$  and of the i.r. transmission data). For comparison the results of the simpler model with an unmodified emissivity [taking  $\varepsilon' = \varepsilon$  in equation (8)], where the coupling of radiation and solid conduction is neglected, have been included in Fig. 3. Especially for low emissivity boundaries ( $\varepsilon = 0.05$ ) the predicted conductivities are about twice as low as the measured ones. This may demonstrate the usefulness of the above introduced effective emissivity  $\varepsilon'$  in combined radiative and conductive heat transfer calculations over a wide range of  $N_1$  values.

## 5. CONCLUSIONS

The heat transfer in silica-aerogel tiles has been studied in detail. Especially the influence of the boundary emissivities and the wavelengths dependent optical thickness on the combined radiative and solid conduction was investigated theoretically and experimentally. Furthermore we could show that for evacuated silica-aerogel installed between low-emissivity envelopes, the reported extremely low apparent thermal conductivities  $\lambda \approx 10^{-2} \text{ W m}^{-1} \text{ K}^{-1}$  not only occur at ambient temperatures ( $T_r \approx 280\text{--}300 \text{ K}$ ) but also up to  $T_r \approx 350 \text{ K}$ . Thus not only windows or covers for low temperature passive solar systems

could be superinsulated with transparent aerogel but also evacuated solar collectors with about  $100^\circ\text{C}$  plate or pipe temperatures.

As the extinction coefficient within the radiative 'window' influences the insulating properties of aerogel severely, it will be necessary to study the influence of adsorbed water more closely.

**Acknowledgements**—The authors are grateful to the aerogel group in Lund (G. v. Dardel and S. Henning) for generously providing us with aerogel and to H. Reiss, Brown, Boverie & Cie., Heidelberg, for making available the radiation thermometer and spectral transmission data of fumed silica.

## REFERENCES

1. M. Rubin and C. M. Lampert, Transparent silica aerogel for window insulation, *Sol. Energy Mater.* **7**, 393–400 (1983).
2. D. Büttner and J. Fricke, Thermal conductivity of evacuated highly transparent silica aerogel, Report E12-0784-1, Physikalisches Institut, Universität Würzburg, F.R.G. (1984). D. Büttner and J. Fricke, Thermal conductivity of evacuated highly transparent silica aerogel, *Int. J. Sol. Energy* **3**, 89–94 (1985).
3. R. Caps and J. Fricke, Radiative heat transfer in highly transparent silica aerogel, Report E12-1283-1, Physikalisches Institut, Universität Würzburg, F.R.G. (1983). R. Caps and J. Fricke, Determination of the radiative heat transfer in transparent silica aerogel, *Int. J. Sol. Energy* **3**, 13–18 (1984).
4. P. Scheuerpflug, R. Caps, D. Büttner and J. Fricke, Apparent thermal conductivity of evacuated SiO<sub>2</sub>-aerogel tiles under variation of radiative boundary conditions, Report E12-1284-1, Physikalisches Institut, Universität Würzburg, F.R.G. (1984).
5. D. Büttner, J. Fricke, R. Krapf and H. Reiss, Measurements of the thermal conductivity of evacuated load-bearing, high temperature powder and glass board insulations, *High Temp.—High Press.* **15**, 233–240 (1983).
6. D. Büttner, J. Fricke and H. Reiss, Thermal conductivity of evacuated load bearing powder and fiber insulations—measurements with the improved  $700 \times 700 \text{ mm}^2$  variable load guarded hot plate device, 9th ETPC, Manchester (1984), to be published in *High Temp.—High Press.*
7. R. Viskanta and R. J. Grosh, Effect of surface emissivity on heat transfer by simultaneous conduction and radiation, *Int. J. Heat Mass Transfer* **5**, 729–734 (1962).
8. W. W. Yuen and L. W. Wong, Heat transfer by conduction and radiation in an one-dimensional absorbing, emitting and anisotropically scattering medium, *J. Heat Transfer* **102**, 303–307 (1980).
9. H. Pöltz, Die Wärmeleitfähigkeit von Flüssigkeiten II—Der Strahlungsanteil der effektiven Wärmeleitfähigkeit, *Int. J. Heat Mass Transfer* **8**, 515–527 (1965).
10. L. S. Wang and C. L. Tien, A study of various limits in radiation heat transfer problems, *Int. J. Heat Mass Transfer* **10**, 1327–1338 (1967).
11. H. C. Hottel and A. F. Sarofim, *Radiative Transfer*. McGraw-Hill, New York (1967).

# CONDUCTIVITE THERMIQUE APPARENTE DE TUILES $\text{SiO}_2$ -AEROGEL SOUS DES CONDITIONS AUX LIMITES RADIATIVES VARIABLES

**Résumé**—La conductivité thermique apparente  $\lambda$  de tuiles  $\text{SiO}_2$ -Aérogel est mesurée avec le système à vide LOLA II, de la petite plaque de garde. De façon à étudier l'influence de l'émissivité de la frontière sur  $\lambda$ , les plaques ( $20 \times 20 \text{ cm}^2$ ) sont utilisées avec leurs surfaces soit revêtues par plasma ( $\varepsilon \approx 0,5$ ), soit couvertes par des feuilles d'aluminium à faible émissivité ( $\varepsilon = 0,05$ ). La différence de conductivité apparente est constatée à la température ambiante et elle augmente d'environ 50% pour les températures radiatives  $T_r = 500 \text{ K}$ . Une conséquence importante est que les systèmes superisolés  $\text{SiO}_2$ -Aérogel doivent toujours être fournis avec des frontières à faible émissivité autour de l'aérogel. Les résultats calorimétriques pour  $\lambda$  sont comparés avec les valeurs de conduction radiative dérivées des mesures de transmission spectrale IR.

# WÄRMELEITFÄHIGKEIT VON EVAKUIERTEN $\text{SiO}_2$ -AEROGEL KACHELN UNTER VARIATION DER BERANDUNGSEMISSIVITÄTEN

**Zusammenfassung**—Die effektive Wärmeleitfähigkeit  $\lambda$  von evakuierten  $\text{SiO}_2$ -Aerogel-Kacheln wurde mit unserer kleinen evakuierbaren Zweiplattenapparatur LOLA II vermessen. Um den Einfluß der Berandungsemissivitäten auf  $\lambda$  zu analysieren, wurden die Meßplatten entweder mit ihren Plasma-gespritzten Oberflächen (Emissivität  $\varepsilon \approx 0,5$ ) eingesetzt oder mit Aluminiumfolien ( $\varepsilon \approx 0,05$ ) abgedeckt. Unterschiede in  $\lambda$  zeigten sich schon bei Zimmertemperatur; sie wuchsen bei Strahlungstemperaturen  $T_r = 570 \text{ K}$  auf etwa 50% an. Eine wichtige Konsequenz hieraus ist, daß superisolierende  $\text{SiO}_2$ -Aerogel-Systeme Berandungen mit kleinem  $\varepsilon$  aufweisen sollten. Die kalorimetrischen  $\lambda$ -Messungen wurden mit Werten für die Strahlungsleitfähigkeit verglichen, die aus spektralen IR-Transmissionsuntersuchungen gewonnen wurden.

# ЭФФЕКТИВНАЯ ТЕПЛОПРОВОДНОСТЬ ВАКУУМИРОВАННЫХ ПЛИТОК, ИЗГОТОВЛЕННЫХ ИЗ ОКСИ КРЕМНИЯ И АЭРОГЕЛЯ, ПРИ ИЗМЕНЕНИИ РАДИАЦИОННЫХ УСЛОВИЙ НА ГРАНИЦЕ

**Аннотация**—С помощью небольшой вакуумной системы LOLA II с защищенной горячей пластиной измерялась эффективная теплопроводность  $\lambda$  вакуумированных плиток, изготовленных из окиси кремния и аэрогеля. Для изучения влияния на  $\lambda$  излучательной способности границы использовались пластины ( $20 \times 20 \text{ см}^2$ ) с поверхностью, либо покрытой плазменным напылением ( $\varepsilon \approx 0,5$ ), либо агюминиевой фольгой, обладающей низкой излучательной способностью ( $\varepsilon \approx 0,05$ ). Показано, что при комнатной температуре эффективная теплопроводность на 50% меньше соответствующей величины для радиационной температуры ( $T_r = 570 \text{ K}$ ). Важным следствием является то, что суперизолированные системы окись кремния-аэрогель должны иметь границы вокруг аэрогеля с низкой излучательной способностью. Калориметрические данные для  $\lambda$  сравниваются со значениями радиационной проводимости, полученными для результатов измерения спектрального пропускания инфракрасного излучения.